PHYSICAL REVIEW E VOLUME 49, NUMBER 6 JUNE 1994

Fast thermalization in supercritical fluids

M. Bonetti, F. Perrot, and D. Beysens
Service de Physique de l'Etat Condensé du Commissariat à l'Energie Atomique, Centre d'Etudes de Saclay, F-91191 Gif-sur-Yvette Cedex, France

Y. Garrabos
Laboratoire de Chimie du Solide du Centre National de la Recherche Scientifique, Université de Bordeaux I, 351, Cours de la Libération, 33405 Talence Cedex, France

(Received 24 January 1994)

Heat transport in supercritical fluids in the absence of gravity is shown to occur in a novel and fast manner. Interferometric observations of the heat transport in supercritical CO_2 at different densities and temperatures around the critical point show two interrelated mechanisms. A diffusing thermal boundary layer and fast adiabatic density increase in the bulk fluid via propagation of pressure waves have been evidenced. The border of the expanding thermal layer acts as a piston. The growth of the thermal boundary layer can be described using a simple scaled function and the bulk density increase is shown to be an adiabatic process. Near the critical point, the diffusing boundary layer can become unstable.

PACS number(s): 44.10.+i, 05.70.Jk, 66.10.Cb

Supercritical fluids, i.e., at pressures and temperatures above the critical point, exhibit specific behavior that makes them attractive for both fundamental science (the critical point is an example of an Ising-like second order phase transition) and industrial applications (for instance, supercritical storage of oxygen and hydrogen is used on board spacecrafts). In such compressible fluids the diffusion of heat is slow which makes them very sensitive to even minute temperature gradients on earth (the Rayleigh number is very large [1]). Thermalization is then ensured by convective flows, mostly turbulent. When gravity is suppressed, one might expect the transport of heat to be performed by diffusion only, which should be very slow, especially near the critical point thanks to the well-known "critical slowing-down."

However, because of the strong divergence of the isothermal compressibility (K_T) near the critical temperature (T_c), a "speeding-up" of the heat transport was recently noticed [2–7]. The mechanism which gives rise to this effect, referred to here as the piston effect (PE), is detailed in numerical simulations [8]. When a wall of an adiabatic cell is instantaneously heated, a thermal boundary layer expands and acts as a "piston," thereby generating acoustic waves which propagate in the bulk. This mechanism leads to an adiabatic increase of the pressure throughout the remaining volume of the (closed) fluid sample. Thermal conversion of the pressure waves results in a spatially uniform increase of the temperature within the bulk fluid on a time scale comparable to a few acoustic times t_s ($t_s = L/c$, with L a characteristic length of the cell and c the sound velocity in the fluid). As first introduced by Onuki and Ferrell [9], the typical time of the transport is $t_c = t_D/(\gamma - 1)^2$. Here, $t_D = L^2/D_t$ is the diffusive time, D_t is the thermal diffusivity, and $\gamma = c_p/c_v$ is the ratio of the specific heats c_p and c_v at, respectively, constant pressure and volume. The time t_c can be understood as the time which is necessary to transfer heat from the diffusive boundary layer, of size δ, into the bulk (size $L-\delta$). This interpretation gives both δ and t_c by noting that equilibration is obtained when the temperature of the bulk has reached that of the diffusive layer. This, in terms of energy, yields in a simplified one dimensional model: $c_p\delta \approx c_v L$, the left hand term corresponding to the energy which has diffused in the boundary layer and has been transferred adiabatically in the bulk. One infers $\delta \approx L/\gamma$ and $t_c = \delta^2/D_t \approx t_D/\gamma^2$. Near T_c, γ diverges and therefore δ and t_c go to 0.

We report, in the following, quantitative interferometry experiments performed under microgravity conditions when the PE is active. Although the PE could be efficient in some way even in the presence of convections, which alter the diffuse boundary layer, experiments under microgravity appear a necessary first step to unambiguously probe the PE mechanisms. The evolution of a thermal boundary layer and the corresponding thermal response of the bulk fluid is investigated in CO_2 fluid at different values of density, temperature, and pressure. We find that the bulk fluid is rapidly heated on the scale t_s as the layer develops and the boundary layer thickness scales with δ and t_c.

Experiment. Sample cells were filled with CO_2 (Air Liquide, purity better than 99.998%) at a critical density $\rho_c = 467.9$ kg/m^3 and at two off-critical densities $\rho = \rho_c \pm 0.18\rho_c$ with an accuracy better than 0.1%. The critical temperature and pressure are 304.14 K and 7.37 MPa. The cells are cylindrically shaped with inner diameter $\Phi = 11.6$ mm and thickness $e = 6.8$ mm as measured between the two windows, made of sapphire. The cells are milled within parallelepipedic copper beryllium blocks of external dimensions $17 \times 24 \times 27$ mm^3 and with thermal diffusivity $D = 3.5 \times 10^{-5}$ m^2 s^{-1}. We estimate the typical diffusive time constant of the cell body to be 1 s. Each cell is mounted into one arm of a Twymann-Green interferometer located at the top of a cylinder made of electrolytical copper with thermal time constant comparable to that of the sample cell. The

cylinder is the central part of a high precision thermostat with a temperature stability better than 50 μK over several hours and spatial temperature gradients less than 100 μK/cm. The temperature of the cylinder is measured and controlled by two Yellow Springs Instrument Co. (YSI) 44900 thermistors screwed into the copper wall near the fluid cell.

Experiments were performed by using two identical thermistors with nearly spherical shape (Thermometrics, B35 PB 103 F-A with time constant of 100 ms and radius $r_{th} = 0.45$ mm) located in the fluid cell at an equal distance from the sapphire windows. The distance between their centers ($L_1 = 4.6$ mm) is comparable to the distance $L_2 = 3.5$ mm between the thermistor center and the cell walls and is close to the half-distance between the inner windows ($e/2 = 3.4$ mm). Only one thermistor (referenced herein as Th1) is used to locally heat the fluid. Th1 delivers directly into the fluid a quantity of heat which depends on the thermistor's resistance and hence on its temperature. In the present study, the delivered power varies between 10 and 80 mW due to Th1 self-heating. During heating, no temperature measurement is available on either thermistor. After heating, Th1 measures the temperature decrease of the thermal boundary layer while Th2 measures the temperature in the bulk fluid. This bulk temperature relaxation process will be the object of a separate analysis [10].

At equilibrium with homogeneous density, the interference fringes (40 fringes in the pattern) are straight and parallel. Density changes in the bulk or at the cell walls result in a refractive index variation and fringes are shifted and/or distorted. Density and refractive index are related through the Lorentz-Lorenz relation [11]. Interference patterns are detected by a two-dimensional (2D) charge-coupled-device (CCD) camera.

Observation. When the heating time on earth exceeds 100 ms (Th1 time response), a convective plume settles in the fluid which destroys the thermal boundary layer around Th1 [Figs. 1(a) and 1(b)]. In microgravity experiments, we limit the heating time to within 20 s, a time which is larger or comparable to t_c (except for the liquid density at $T_c + 17.1$ K, see Table I) but much larger than t_s. Results obtained using larger times are difficult to interpret because the radius r_b of the thermal layer approaches a size comparable to $e/2$ and the cell walls constrain the growth of the boundary layer. Figures 1(a), 1(c), and 1(d) show a growth sequence under microgravity conditions (mean value of order $10^{-5}g$ and g jitter $< 10^{-4}g$). No convective plume is observed. Instead, a thermal boundary layer whose shape follows that of the thermistor develops around it.

The thermal layer appears as a black region where fringes are not visible, with a well-defined border. Outside the border, in the bulk, the fringes are not distorted and remain straight. During heating we observe both a growth of the boundary layer and a shift of the whole bulk fringe pattern, with the fringes remaining straight. A simulation of the fringe pattern shows that for a fringe spacing $\lambda < \lambda_0/4$ ($\lambda_0 = 0.3$ mm as in the experiment) the fringe visibility is strongly reduced for a spherical density inhomogeneity of order 1%. This confirms that the thermal layer is a region of large density—and hence temperature—gradients. The instantaneous translation of the fringes pattern with constant spacing corresponds to a spatially *uniform* density change throughout the entire cell, the signature of the piston effect.

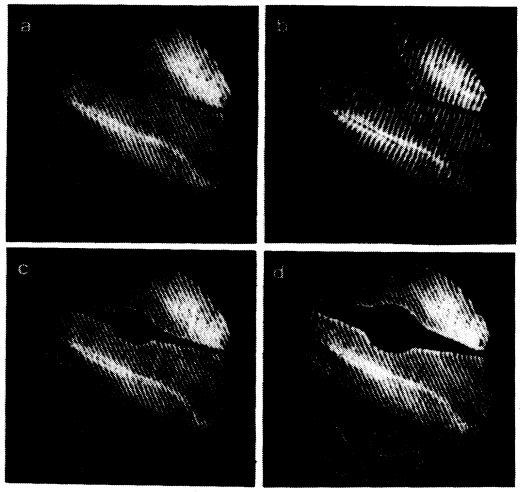

FIG. 1. Evolution of a thermal boundary layer around a heating thermistor (CO_2 at $\rho = \rho_c$). (a) Before heating. View of the cell with both thermistors. The cell is 11.6 mm diameter. The two spheres are thermistors. The lines are interference fringes. (b) Experiment under earth's gravity ($T = T_c + 16$ K, $t = 400$ ms after heating has started). Notice the convective plume. (c) Experiment under microgravity ($T = T_c + 16.8$ K, $t = 400$ ms after heating has started). (d) The same as in (c) at $t = 2$ s.

Discussion. We have analyzed the layer growth in the framework of the theory by Onuki and co-workers [9]. In this theory (1D model), after a fast temperature increase at the wall, the bulk temperature is expected to increase within the characteristic time t_c as defined above and the typical thickness e_b of the diffusing boundary layer should be of order δ. It is assumed that δ is much smaller than the cell size and the reduced thickness $e^* = e_b/\delta$ varies with reduced time $t^* = t/t_c$ as $A(t^*)^\alpha$ where $A = 1.13$ and $\alpha = 0.5$. In our experiment the layer thickness $e_b = r_b - r_{th}$, measured perpendicularly to the thermistor wires [see Fig. 1(a)], scales with

$$\delta = \frac{e}{2}\frac{1}{(\gamma-1)}, \quad t_c = \frac{e^2}{4}\frac{1}{D_t}\frac{1}{(\gamma-1)^2}.$$

TABLE I. Characteristic time t_c as a function of temperature $\Delta T = (T - T_c)$ at critical and off-critical densities.

ΔT (K)	−0.03	0.0	0.2	0.67	0.7	1.0	16.77	16.8	17.1
$\rho = \rho_c$			0.07 s			0.73 s		20.22 s	
$\rho = \rho_c - 0.18\rho_c$	18.2 s			22.6 s			36.5 s		
$\rho = \rho_c + 0.18\rho_c$		24.6 s			30.1 s				113.6 s

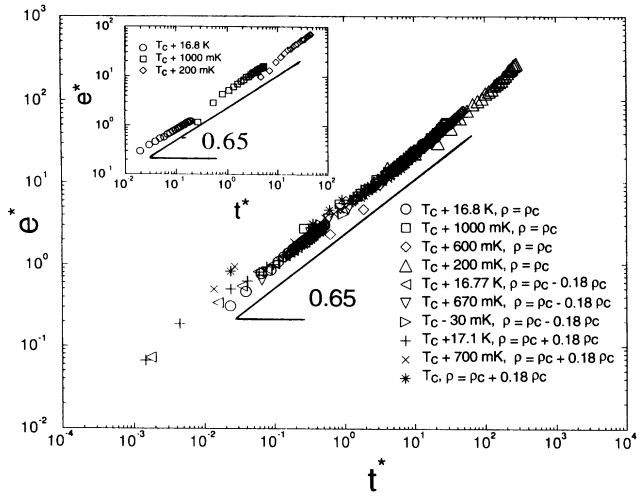

FIG. 2. Reduced thickness e^* of the thermal boundary layer as a function of the reduced time t^* (see text) at $\rho = \rho_c$ and $\rho = \rho_c \pm 0.18\rho_c$ and for different temperatures. Fluid temperature is relative to T_c and always above the coexistence curve. Inset: Normalized time evolution of the thermal boundary thickness computed from a purely diffusive process at $\rho = \rho_c$.

Figure 2 shows a log-log plot of the reduced thickness e^* versus the reduced time t^* at $\rho = \rho_c$ and $\rho = \rho_c \pm 0.18\rho_c$. All data lie on a single line with exponent α close to 0.65 and $A \approx 5$. Note that scaling extends to a thickness e_b as large as 1000δ and is valid in the whole supercritical region. In the inset we also report the evolution of a purely diffusive layer around a heating sphere in an infinite incompressible medium with constant diffusivity. The radial temperature profiles from which the thermal boundary layer thickness is determined are computed from the analytical solution given in Ref. [12]. The estimated boundary layer thickness is the radius at which the temperature profile corresponds to a density inhomogeneity of order 1% compared to the bulk density. Outside the estimated boundary layer, the temperature profiles show weak spatial gradients. Therefore scaling in time with t_c and in space with δ can be used according to Onuki and co-workers' theory where it is assumed that the bulk fluid has a spatially uniform temperature. The same behavior as above for the experimental data is obtained. Indeed, a power law with $\alpha \simeq 0.65$ holds. This confirms that the observed thermal layer around the thermistor is governed by a diffusion process and the value of the exponent $\alpha \simeq 0.65$ is related to the 3D geometry compared to the 1D case where $\alpha = 0.5$.

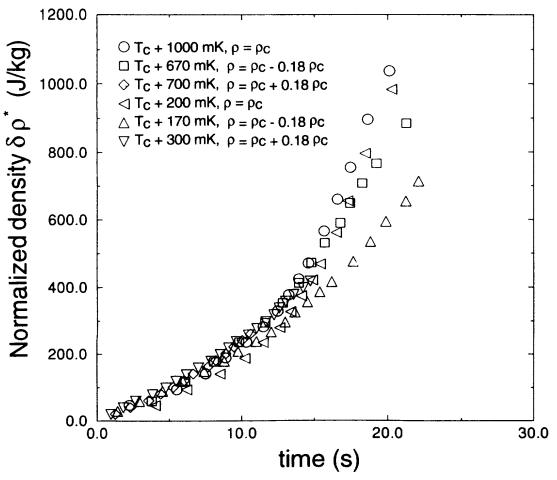

FIG. 3. Normalized density increase $\delta\rho^*$ (see text) in the bulk fluid as a function of time.

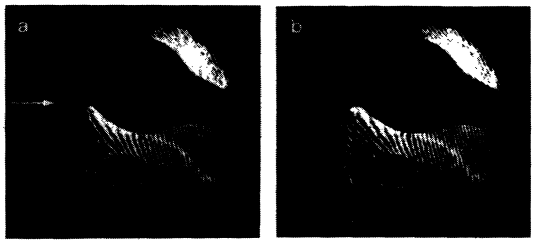

FIG. 4. "Burst" of the thermal boundary layer ($T = T_c + 200$ mK). Notice the vortex shape of the ejection indicated by the white arrow. (a) $t = 0.4$ s after the starting of the ejection, (b) $t = 1.4$ s.

The bulk density evolution is measured by means of the fringe shift. The relative density variation per fringe is $\simeq 0.04\%$. This shift is counted as the number of fringes which cross a reference line parallel to the initial fringe orientation. When the fluid (mass M) receives the energy amount E, the density increase in the bulk due to adiabatic heating is given by

$$\delta\rho = \left(\frac{\partial\rho}{\partial T}\right)_p \frac{1}{(\gamma-1)c_v}\frac{E}{M} = R\frac{E}{M}.$$

In Fig. 3 we compare the density variations in the bulk normalized to R ($\delta\rho^* = \delta\rho/R$). All the curves collapse on one single curve for $t < 10$ s [13]. The time variation of $\delta\rho^*$ is not simple to analyze because of the thermistor self-heating phenomenon which makes the heating power increasing with time. It is interesting to note that, while the density is decreasing in the boundary layer, it increases in the bulk, thus making true the image of a "piston"—the boundary layer border—pressurizing the rest of the fluid. Note that since we have an adiabatic process, the uniformity of the bulk density corresponds to a uniform bulk temperature.

A striking phenomenon of instability was observed at the surface of the boundary layer during its growth. A jet of inner fluid is sent into the bulk fluid [Figs. 4(a) and 4(b)]. The ejection mechanism is randomly positioned at the surface and has a vortex shape with an initial ejection speed estimated to be 1 cm/s. During this phenomenon no acceleration perturbation was observed.

This work was supported by Centre National d'Etudes Spatiales (CNES). The experiments were performed in the laboratory "Analyses des Liquides Critiques dans l'Espace" (ALICE) [14] on board the orbital station MIR (ANTARES mission). We are particularly indebted to P. Koutsikides and J. M. Laherrère from the ALICE project. We thank B. Zappoli, P. Carlès, and A. Onuki for fruitful discussions.

[1] J. V. Sengers, in *Critical Phenomena*, Proceedings of the International School of Physics "Enrico Fermi," Course LI, edited by M. S. Green (Academic, New York, 1971), p. 445.

[2] A. M. Radhwan and D. R. Kassoy, J. Eng. Math. **18**, 133 (1984).

[3] K. Nitsche and J. Straub, Naturwissenschaften **73**, 370 (1986).

[4] R. P. Behringer, A. Onuki, and H. Meyer, J. Low Temp. Phys. **81**, 71 (1990).

[5] H. Boukari, M. E. Briggs, J. N. Shaumeyer, and R. W. Gammon, Phys. Rev. Lett. **65**, 2654 (1990).

[6] H. Klein, G. Schmitz, and D. Woerman, Phys. Rev. A **43**, 4562 (1991).

[7] P. Guenoun, B. Khalil, D. Beysens, Y. Garrabos, F. Kammoun, B. Le Neindre, and B. Zappoli, Phys. Rev. E **47**, 1531 (1993).

[8] B. Zappoli, D. Bailly, Y. Garrabos, B. Le Neindre, P. Guenoun, and D. Beysens, Phys. Rev. A **41**, 2264 (1990).

[9] A. Onuki and R. A. Ferrell, Physica A **164**, 245 (1990); A. Onuki, H. Hao, and R. A. Ferrell, Phys. Rev. A **41**, 2256 (1990).

[10] M. Bonetti, F. Perrot, D. Beysens, and Y. Garrabos (unpublished).

[11] M. Born and E. Wolf, *Principles of Optics*, 6th ed. (Pergamon, New York, 1980).

[12] H. S. Carslaw and J. C. Jaeger, *Conduction of Heat in Solids*, 2nd ed. (Oxford University Press, London, 1959).

[13] Although the temperatures are not exactly the same for critical and off-critical data, the values of the normalization parameters R do not differ more than 0.7%.

[14] J.-M. Laherrère and P. Koutsikides, Acta Astronaut. **29**, (10/11), 861 (1993).

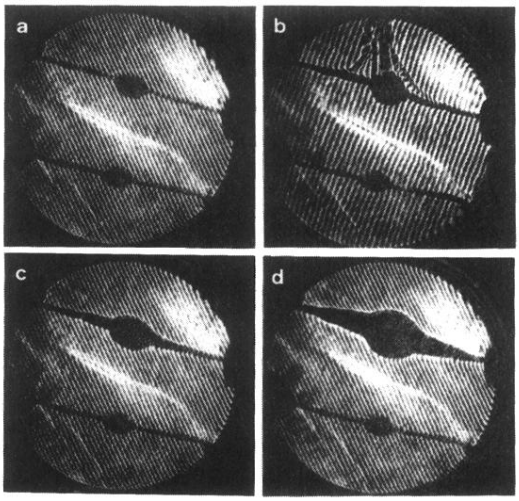

FIG. 1. Evolution of a thermal boundary layer around a heating thermistor (CO_2 at $\rho = \rho_c$). (a) Before heating. View of the cell with both thermistors. The cell is 11.6 mm diameter. The two spheres are thermistors. The lines are interference fringes. (b) Experiment under earth's gravity ($T = T_c + 16$ K, $t = 400$ ms after heating has started). Notice the convective plume. (c) Experiment under microgravity ($T = T_c + 16.8$ K, $t = 400$ ms after heating has started). (d) The same as in (c) at $t = 2$ s.

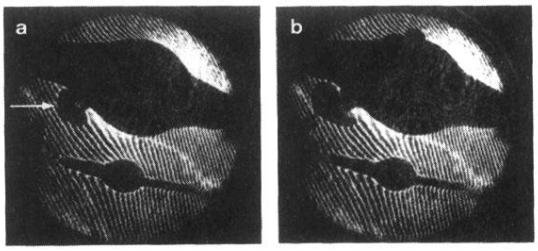

FIG. 4. "Burst" of the thermal boundary layer ($T = T_c + 200$ mK). Notice the vortex shape of the ejection indicated by the white arrow. (a) $t = 0.4$ s after the starting of the ejection, (b) $t = 1.4$ s.